

Density of states determined from Monte Carlo simulations

J. Hove*

Bergen Centre for Computational Science
5020 Bergen

(Dated: March 25, 2019)

We present a novel method for calculation of Density of States $g(\epsilon)$ from Monte Carlo simulations. We discuss how critical properties reveal themselves in $g(\epsilon)$ and demonstrate this by applying the method several different phase transitions.

PACS numbers: 05.10.Ln,05.50.+q,64.10+h,75.40.Mg

I. INTRODUCTION

Since it was devised by Metropolis in 1953[1] Monte Carlo (MC) simulations based on the Metropolis algorithm have had a tremendous impact on physics; SIAM recently rated the algorithm among the ten most influential numerical algorithms of the previous century[2]. For a historical summary, and a review of modern MC methods we refer to the proceedings of the conference hosted to celebrate the 50th anniversary of the algorithm[3].

The Metropolis algorithm is well suited to calculate quantities which can be expressed as

$$\langle O \rangle = \frac{1}{N} \sum_i \hat{O} |\psi_i\rangle, \quad (1)$$

i.e. as averages of values obtained by operating an operator \hat{O} on a series of states $|\psi_i\rangle$. Focusing on phase space Eq. 1 can be denoted a *local* estimator, in the sense that only one point in phase space is involved at a time. Some quantities like entropy and free energy can not be expressed like Eq. 1; their evaluation requires simultaneous knowledge of global portions of phase space.

We have devised a post-processing method for Metropolis simulations to obtain $\ln \tilde{g}(\epsilon) = \ln g(\epsilon) + C$, where $g(\epsilon)$ is the density of states, and C is an additive constant. In models with discrete energy distributions and finite ground state degeneracy, like the Ising model, we can determine $\ln g(\epsilon)$ precisely. When we have $\ln g(\epsilon)$ we can easily calculate the free energy, and arbitrary moments of $\langle E \rangle$.

Entropy and free energy can in principle be obtained by thermodynamic integration[4],

$$F(T) = U(T) - T \int_0^T dT' \frac{C_V(T')}{T'}, \quad (2)$$

but this technique does not seem to be much used. Recent modern sampling techniques like e.g. multicanonical sampling provide estimates of the density of states, however these are generally completely different algorithms

designed to overcome the difficulties of a rugged energy landscape or large free energy barriers[5].

The rest of the paper is organised as follows: In section II we present an algorithm to calculate the density of states, $g(\epsilon)$, by combining the results from MC simulations performed at several different couplings. Section III is devoted to a short discussion of statistical mechanics based on $g(\epsilon)$. In the final section IV we apply the algorithm to the several different phase transitions.

II. ESTIMATING $g(\epsilon)$

When doing a MC simulation with the Metropolis algorithm the probability to be in a state ψ with energy ϵ_ψ is proportional to

$$g(\epsilon_\psi) e^{-\beta \epsilon_\psi}. \quad (3)$$

If we record a histogram of energies from a simulation at coupling β ; we get a histogram $h_\beta(\epsilon)$ which is proportional to $g(\epsilon) e^{-\beta \epsilon}$. Multiplying this histogram with $e^{\beta \epsilon}$ we get something which is proportional to $g(\epsilon)$, i.e.

$$\hat{g}_\beta(\epsilon) = e^{\xi \beta} e^{\beta \epsilon} h_\beta(\epsilon) \quad (4)$$

is an estimator for $g(\epsilon)$. In Eq. 4 $e^{\xi \beta}$ is a dimensionless constant of proportionality to be determined. The density of states in Eq. 4 has an index β to indicate that the histogram was recorded at this coupling, but it does not have any intrinsic temperature dependence. In principle Eq. 4 can be used to estimate $g(\epsilon)$ regardless of temperature, however practically only a small energy range around $\langle E \rangle(T)$ will be sampled with a sufficiently high frequency.

Although Eq. 4 is useless as an immediate estimator for $g(\epsilon)$, it provides a basis for *combining* results from different couplings to an estimator $\hat{g}(\epsilon)$ which can be applied over the complete energy range. Given N different histograms $h_i(E)$ recorded at the couplings $\beta_1 > \beta_2 > \dots > \beta_N$, we can combine them as

$$\hat{g}(\epsilon) = g_0 \sum_{i=1}^N \Xi_i h_i(\epsilon) w_i(\epsilon) e^{\beta_i \epsilon}, \quad (5)$$
$$w_i(\epsilon) = \frac{h_i(\epsilon)}{\sum_{i=1}^N h_i(\epsilon)},$$

*Electronic address: hove@bccs.no

to obtain an estimator which is usable over the complete ϵ range $[\min_{\epsilon} h_i(\epsilon), \max_{\epsilon} h(\epsilon)]$. In Eq. 5 $w_i(\epsilon)$ is a weight function, which denotes the weight ascribed to histogram i in the estimation of $g(\epsilon)$. The constants e^{ξ_i} are deter-

mined by joining the various histograms.

The algorithm we have applied to determine ξ_i is to set ξ_1 to an arbitrary value, and then compute $\xi_{i>1}$ by minimizing

$$\chi^2 = \sum_{i=1}^{N-1} \sum_{j=i+1}^N \sum_{\epsilon} h_i(\epsilon) h_j(\epsilon) \underbrace{(\xi_i + \beta_i \epsilon + \ln h_i(\epsilon) - \xi_j - \beta_j \epsilon - \ln h_j(\epsilon))^2}_{\ln \hat{g}_{\beta_i}(\epsilon) - \ln \hat{g}_{\beta_j}(\epsilon)}. \quad (6)$$

As indicated in Eq. 6 the central principle is to minimize the pairwise difference between all the $\hat{g}(\epsilon)$ estimates, where the estimates $\hat{g}_{\beta_i}(\epsilon)$ are given according to Eq. 4. Minimizing χ^2 with respect to ξ_i gives N linear equations which can be solved by e.g. LU decomposition. Actually it turns out that a much simpler algorithm, based on calculating ξ_{i+i} directly from ξ_i gives very similar results. In particular for large N this is much faster.

When the coefficients ξ_i have been determined we have all the coefficients $\xi_{i>1}$ expressed in terms of ξ_1 . For discrete models with a finite ground state degeneracy g_0 we can determine ξ_1 by requiring $g(\epsilon_0) = g_0$. In section IV we will consider both discrete models where the complete normalisation can be achieved, and continuous models where ξ_1 must be left undetermined.

Use of Eq. 5 to determine $g(\epsilon)$ is in principle quite straightforward, but in practice it is important to be careful to avoid numeric underflow or overflow in intermediate steps, in particular the implementation must ensure that only $\ln g(\epsilon)$ is needed in actual computations.

III. STATISTICAL MECHANICS FROM $g(\epsilon)$

Knowledge of $g(\epsilon)$ is in principle equivalent to knowledge of the partition function $Z(\beta)$, hence all the properties of a system are contained in $g(\epsilon)$, however $g(\epsilon)$ does not have a very prominent role in modern statistical mechanics. We will therefor express some important results based on $g(\epsilon)$ in this section, examples/applications are given in section IV. The definition of temperature in statistical mechanics[6], is given by

$$\beta = \frac{\partial \ln g(\epsilon)}{\partial \epsilon}. \quad (7)$$

From this we find that the fundamental requirement $C_V(T) \geq 0$ is equivalent to $\partial_{\epsilon}^2 \ln g(\epsilon) \leq 0$. The limiting value $\partial_{\epsilon} \ln g(\epsilon) = C$ is the signature of a phase transition. A finite ϵ range with $\partial_{\epsilon} \ln g(\epsilon) = C$ means that the temperature is unchanged for this ϵ range, i.e. an indication of a first order transition; actually, as we shall see in section IV B this is slightly more complicated. When the width of the of linear part of $\ln g(\epsilon)$ diminishes the first order transition is weakened; until $\partial_{\epsilon}^2 \ln g(\epsilon) = 0$ in a

isolated point only, this is the manifestation of a critical point. If we differentiate Eq. 7 with respect to T we find the function $C_V(\epsilon)$

$$C_V(\epsilon) = \frac{d\epsilon}{dT} = \frac{-(\partial_{\epsilon} \ln g(\epsilon))^2}{\partial_{\epsilon}^2 \ln g(\epsilon)}. \quad (8)$$

From Eq. 8 we see that the critical properties, and in particular the critical exponent α , must be related to how $\partial_{\epsilon}^2 \ln g(\epsilon)$ approaches zero. To infer α directly from the behaviour of $g(\epsilon)$ close to ϵ_c is difficult, but if we make the size dependence of $g(\epsilon)$ explicit we can use finite size scaling[7]. At the (pseudo)critical point in a finite system, C_V scales as $L^{d+\alpha/\nu}$. The factor $(\partial_{\epsilon} \ln g(\epsilon))^2$ in Eq. 8 is just equal to β_c^2 , hence the critical properties must come from the second derivative

$$|\partial_{\epsilon}^2 \ln g(\epsilon, L)| L^d \propto L^{-\alpha/\nu}. \quad (9)$$

In general $\partial_{\epsilon} \ln g(\epsilon, L)$ will also have finite size effects, however for this only the *deviation* from the thermodynamic value will show critical scaling.

When we have $g(\epsilon)$ we can easily calculate $F(T)$ and $P(\epsilon, T)$

$$F(T) = -T \ln \sum_{\epsilon} g(\epsilon) e^{-\beta \epsilon}, \quad (10)$$

$$P(\epsilon, T) = \frac{g(\epsilon) e^{-\beta \epsilon}}{\sum_{\epsilon} g(\epsilon) e^{-\beta \epsilon}}. \quad (11)$$

From $P(\epsilon, T)$ we can easily calculate the internal energy, and all moments thereof. If we in addition to ϵ sample other operators like the magnetisation, we can use $P(\epsilon, T)$ to find thermal averages of arbitrary operators,

$$\langle O \rangle_T = \sum_{\epsilon} \langle O \rangle_{\epsilon} P(\epsilon, T). \quad (12)$$

In Eq. 12 $\langle O \rangle_{\epsilon}$ is the mean of \hat{O} for a given value of ϵ .

IV. SOME APPLICATIONS

In this section we present various applications of the method presented in the preceding sections. In section

IV A the results are benchmarked against the 2D Ising model, where $F(T)$ has been determined exactly *even for finite systems*[8]. In section IV B we investigate the way phase transitions reveal themselves in $g(\epsilon)$. In section IV C we calculate the finite size corrections to the free energy in a cylindrical geometry. For conformally invariant systems[9] this is universal[10, 11], and can be used to calculate the conformal charge. We have determined the conformal charge for the 2D Ising model, and the 2D $Q = 3$ Potts model. In section IV D we discuss the problems related to models with a continuous energy distribution; and show that method is useful also for these systems, although less so. Finally in section IV E we have applied the method to a large dataset obtained from a previous study of the full Ginzburg Landau (GL) model.

A. Comparisons with exact results

Due to Onsagers exact solution[12] the 2D Ising model has been one of the most used benchmarks in statistical physics. For a rectangular lattice with periodic boundary the model has been solved in closed form even for finite systems[8], this constitutes a very convenient benchmark for our approach. We have performed simulations on a 32×32 system with periodic boundary conditions, and verified that within statistical error both $F(T)$ and $C_V(T)$ agree with the exact values, see figures 1 - 2.

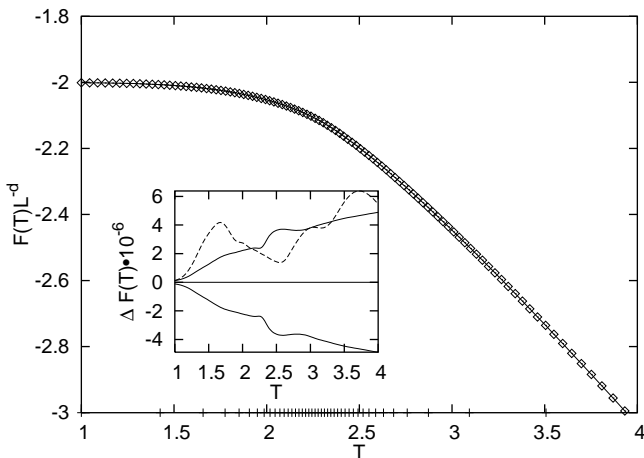


FIG. 1: This figure shows the estimated value of $F(T)$ as symbols, and the exact value from [8] as a solid line. The small ticks on T axis indicate T values were simulations have been performed. In the inset the dashed curve shows the relative error of the estimated values, and the solid lines are \pm an estimated statistical error.

The statistical errors errors indicated on figures 1 and 2 are calculated by performing ten completely independent simulations.

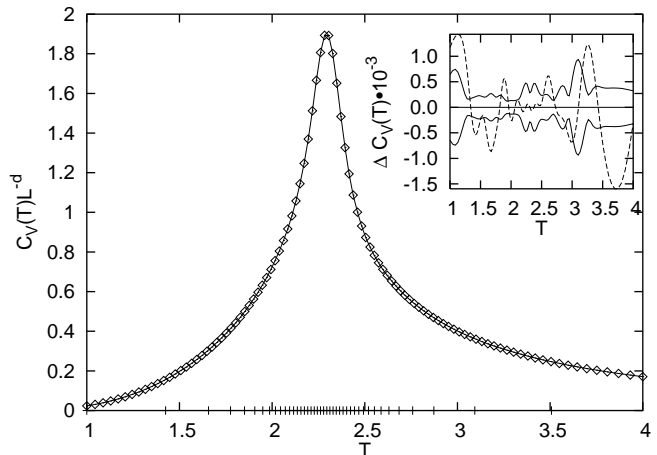


FIG. 2: This figure shows essentially the same as Fig. 1, but for the specific heat $C_V(T)$.

B. The signature of phase transitions in $g(\epsilon)$

As discussed in section III all critical properties must be present in $g(\epsilon)$. In this section we will discuss the critical properties of the $Q = 3$ and $Q = 10$ Potts model. The first model has a continuous phase transition with $\alpha = 1/3$ and $\nu = 5/6$ [13], i.e. $\alpha/\nu = 0.4$, the second model has a first order transition.

First we consider the $Q = 3$ model, for this model the goal is to determine the ratio α/ν from $g(\epsilon, L)$. According to Eq. 9 this can be done by considering how $\partial_\epsilon^2 \ln g(\epsilon, L)$ vanishes when approaching the critical energy ϵ_c . Fig. 3 shows $L^d \partial_\epsilon^2 \ln g(\epsilon, L)$ for different system sizes, and we can see that peak grows closer to zero with increasing system size.

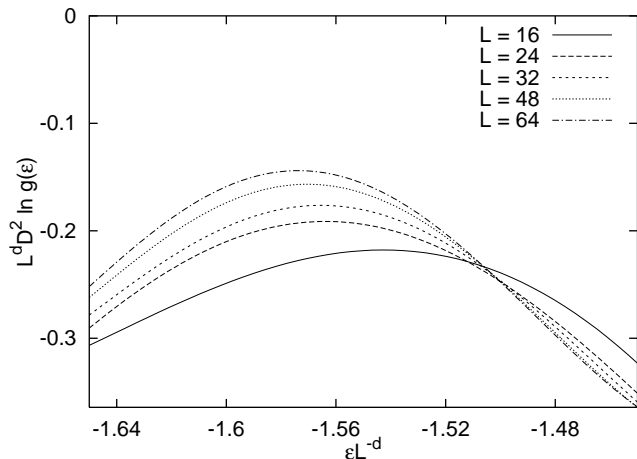


FIG. 3: $L^d \partial_\epsilon^2 \ln g(\epsilon, L)$ for different system sizes, in the limit $L \rightarrow \infty$ this vanishes as $L^{-\alpha/\nu}$.

In Fig. 4 we have plotted $\min |L^d \partial_\epsilon^2 \ln g(\epsilon, L)|$, i.e. the magnitude of the *peak* value for the curves in Fig. 3, as a function of L .

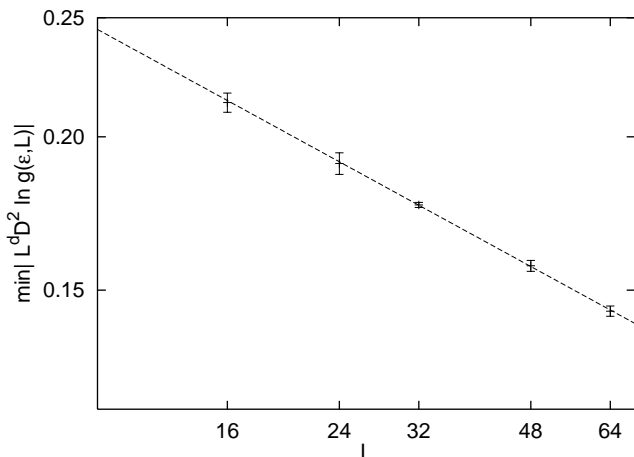


FIG. 4: This shows finite size scaling of $L^d \min |\partial_\epsilon^2 g(\epsilon, L)|$ in a log-log plot, the dashed line has slope $-\alpha/\nu \approx -0.29$.

The dashed line in Fig. 4 has slope of $-\alpha/\nu \approx -0.29$; this is a significant deviation from the exact value $\alpha/\nu = 0.40$, however we feel that these results are sufficient to demonstrate that the critical properties, and in particular the exponents α and ν are contained in $g(\epsilon)$. There is clearly significant finite size effects in $\partial_\epsilon \ln g(\epsilon, L)$ also; including the factor $\partial_\epsilon \ln g(\epsilon)$ gives the “improved” value $\alpha/\nu \approx 0.35$, however this can not contribute in the $L \rightarrow \infty$ limit and we have therefor not included this factor in Fig. 4. Finally Fig. 4 is based on the second derivative of a sampled quantity; hence it will clearly be difficult to determine with high precision. In conclusion it is definitely *possible* to infer the ratio α/ν from the properties of $g(\epsilon, L)$, but it is certainly not the most suitable way for high precision measurements. Finally we mention that the remaining critical exponents can *not* be obtained from $g(\epsilon)$, their value is based on the explicit choice of fields to represent the critical state.

For second order transitions we had to revert to FSS to infer critical properties from $g(\epsilon)$; in the case of first order transitions we can make quite powerful statements from $g(\epsilon)$ alone. Given a first order transition between the pure states ϵ_1 and ϵ_2 the probability $P(\epsilon, T)$ is bimodal, with distinct peaks at the pure energy levels ϵ_1 and ϵ_2 . The mixed states with energy $\epsilon_1 < \epsilon < \epsilon_2$ are exponentially suppressed, to reproduce this behaviour we must have

$$\ln g(\epsilon_1 + \Delta\epsilon) < \ln g(\epsilon_1) + \beta \ln \left(\frac{g(\epsilon_1 + \Delta\epsilon)}{g(\epsilon_1)} \right). \quad (13)$$

for $0 < \Delta\epsilon < \epsilon_2 - \epsilon_1$. Hence $\ln g(\epsilon)$ must increase *weaker* than linearly in the immediate vicinity of ϵ_1 and then subsequently stronger than linearly afterwards such that the relation $\beta_c = \partial_\epsilon \ln g(\epsilon_1) = \partial_\epsilon \ln g(\epsilon_2)$ is satisfied. If we insist on $\partial_\epsilon^2 \ln g(\epsilon) \leq 0$ also in the interval $\epsilon_1 < \epsilon < \epsilon_2$ $\ln g(\epsilon)$ must have a *cusplike* in this interval; however these energy levels correspond to states which are manifest not equilibrium so maybe it does not make sense to require

$\partial_\epsilon^2 \ln g(\epsilon) \leq 0$ in this particular interval?

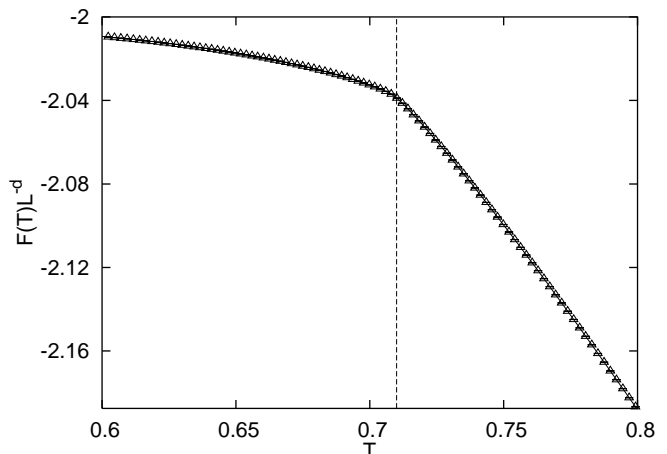


FIG. 5: The free energy $F(T)$ for the $Q = 10$ Potts model which has a strong first order transition. Although there is inevitably some finite size rounding, the cusp in this figure is quite clear. Fig. 1 shows a similar figure for a continuous transition, this clearly smooth in comparison.

C. Conformal charge

It is well known that critical systems are *scale invariant*; in addition the critical systems often possess further symmetries like translational and rotational invariance. Together these operations form a group \mathcal{G} . Under quite mild restrictions, in particular finite length interactions, the system is actually invariant also under transformations which *vary in space*, this means that \mathcal{G} is the conformal group. In particular for $d = 2$ this is a very powerful result, and the application of Conformal Field Theory (CFT) has lead to many exact results for the critical state[14].

Consider an infinitely long strip of width W , due to the finite width there will be finite size corrections to the free energy density. One of the most fundamental results from conformal invariance is that the leading finite size correction for this system is universal[10, 11]

$$f_W = f_B - \frac{\pi c}{6W^2} + \mathcal{O}\left(\frac{1}{W^4}\right). \quad (14)$$

In Eq. 14 f_W is the free energy density of the strip, f_B is the bulk free energy density of an infinite system and c is the conformal charge or anomaly. The conformal charge is a dimensionless number which uniquely characterises a given universality class. In two dimensions the Ising model has $c = 0.5$ and the $Q = 3$ Potts model has $c = 0.8$ [9].

Eq. 14 is a finite size scaling expression which should be very useful for numeric evaluation of c . However, since the use of Eq. 14 requires knowledge of the free energy

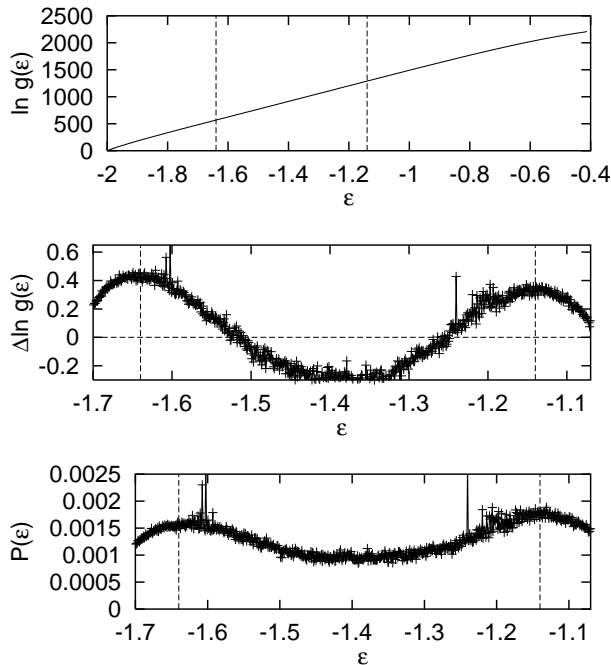


FIG. 6: The uppermost panel shows $\ln g(\epsilon)$, the two dashed lines indicate the two energy levels ϵ_1 and ϵ_2 . The central panel shows $\ln g(\epsilon) - [\beta(\epsilon - \epsilon_1) + \ln g(\epsilon_1)]$, which clearly shows that $\ln g(\epsilon)$ has small but significant deviations from perfect linearity in the range $\epsilon_1 < \epsilon < \epsilon_2$. The bottom panel shows $P(\epsilon, T_c)$, i.e. Eq. 11 at the critical point, and we can clearly see how the depression in $P(\epsilon, T_c)$ originates from the features in $\ln g(\epsilon)$.

MC has not been extensively used; see however for instance [15] for a numerical test of another Conformal Field Theory conjecture by MC methods. The numerical evaluation of c has been dominated by transfer matrix methods[9, 16].

Using the method presented in this paper we have calculated c for the Ising model and the $Q = 3$ Potts model. We have considered cylindrical systems of length L and circumference W , we have considered $W = \{4, 5, 6, 8, 10, 12, 16\}$, and for each W we have used $L = \{W, 2W, 4W, 8W, (16W)\}$, $L = 16W$ was only considered for the Ising model. From this we have extrapolated to find

$$f_W = \lim_{L \rightarrow \infty} \frac{1}{LW} F(L, W). \quad (15)$$

Plots of f_W are shown in Fig. 7, and c has been determined from a least squares fit to these curves. The curves in Fig. 7 show that there are quite significant corrections to the W^{-2} term for small W , and the numerical results $c = 0.49 \pm 0.07$ for the Ising model was obtained by excluding all $W < 8$. Including an additional fourth order term[16], and including all the results we get $c = 0.55 \pm 0.06$. Most of the computational resources were spent on the Ising model, and the $Q = 3$ Potts results are lower quality, the solid line corresponds to $c = 0.86 \pm 0.19$,

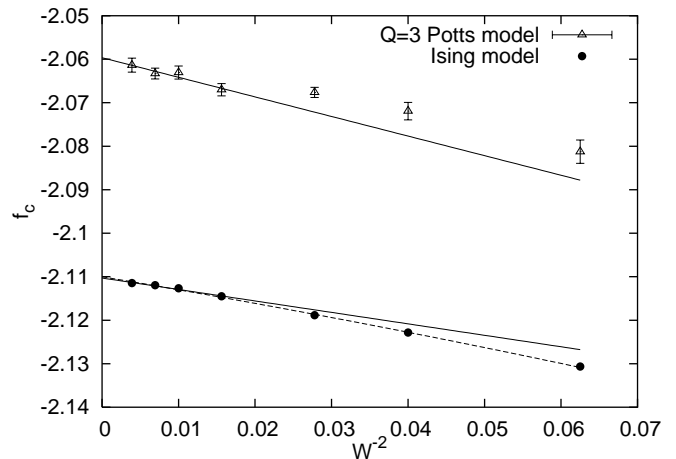


FIG. 7: The extrapolated limit f_W from Eq. 15 for the Ising and $Q = 3$ Potts model. The conformal charge is given by the slope in the $W^{-2} \rightarrow 0$ limit. The solid line is a least squares fit to Eq. 14 and the dashed line comes from including an additional term αW^{-4} in the fit. For the Ising model the error bars are smaller than the symbol size.

this was obtained by retaining only the four largest W values.

D. Continuous systems

The method we have presented can to some extent also be applied to systems with a continuous energy distribution, however for these systems the full normalisation of $g(\epsilon)$ is difficult. The method used to normalise $g(\epsilon)$ for discrete systems so far require that (i) the ground-state is sampled, and (ii) that the histograms have sufficient overlap. For a system with a truly continuous energy distribution sampling of the ground-state requires $T \equiv 0$, and this will generate histograms without overlap. Even for models with a very small energy gap, like e.g. the Z_q [17] model for large q a large fraction of the computational resources must be spent close to the ground state to ensure that both the conditions are met. Attempts to generalise the Wang Landau histogram sampling to continuous systems are faced with essentially the same problems[18].

Due to the problems with normalisation we must generally be content with a function $\ln \tilde{g}(\epsilon) = \ln g(\epsilon) + \mathcal{C}$ where \mathcal{C} is an unknown, dimensionless constant. This will induce a linear error $\Delta F(T) = -T \ln \mathcal{C}$ in the free energy, but since Eq. 11 is independent of \mathcal{C} all remaining thermodynamics will be unaffected by the incomplete normalisation.

The Z_q clock model is a planar spin model where the real angle $\phi \in [0, 2\pi)$ is approximated with the discrete variable $\theta_i = i2\pi/q$, in the limit $q \rightarrow \infty$ the converges to the XY model. Numerical simulations of the XY model are customarily done using the Z_q model with q “large

enough”, values of $q = 32$ or 64 are often used. Furthermore it has been shown that already at $q = 5$ the critical properties are governed by the XY critical point[17, 19]. To learn about the behaviour $g(\epsilon)$ for continuous systems we have done a short simulation of a 32×32 system for the Z_q model with $q = 2048$, according to the discussion above this should with a good capture the properties of the continuous $q \rightarrow \infty$ system. Fig. 8 shows $\ln g(\epsilon)$ for the Z_q model with $q = 2048$ along with the Ising model.

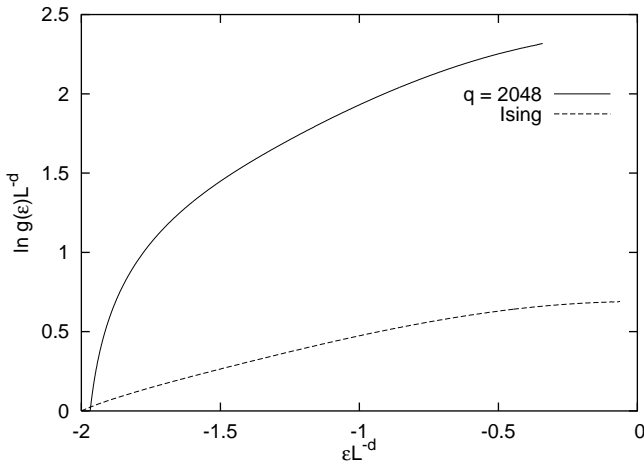


FIG. 8: Comparison of $\ln g(\epsilon)$ for the $q = 2048$ Z_q model and the Ising model. Observe that the curve for the Z_q model has been vertically shifted by an *unknown* amount, see text.

For the Z_q model the lowest lying of the sampled states has energy ϵ_- , hence the Z_q curve in Fig. 8 terminates at this ϵ value. This means that $g(\epsilon)$ is undetermined in the interval $[\epsilon_0, \epsilon_-)$, where $\epsilon_0 = -2L^d$ is the ground-state energy. Furthermore overall normalisation is impossible to determine, and we have just arbitrarily fixed $\ln g(\epsilon_-) = 0$.

According to Eq. 11 internal energy and specific heat depend only on the shape of $\ln g(\epsilon)$, and not possible vertical offset. Combined with the knowledge from previous simulations: that the Z_q model for large q correctly captures the thermodynamics of the XY model, we can conclude that apart from the vertical offset Fig. 8 is a faithful representation of $g(\epsilon)$ for the continuous XY model. Looking at Fig. 8 the most striking features are (i) $g(\epsilon)$ is orders of magnitude larger for the Z_q model than the Ising model, and (ii) the steep slope of $\ln g(\epsilon)$ for the Z_q model; actually any gap-less model must have $\lim_{\epsilon \rightarrow \epsilon_0} \partial_\epsilon g(\epsilon) \rightarrow \infty$ to produce a finite value for $C_V(T)$ in the limit $T \rightarrow 0$.

In section IVE we will reanalyse a real dataset from a large scale simulations of the Ginzburg Landau model, this constitutes a real example of a continuous system.

E. Reanalysing Ginzburg Landau results

The Ginzburg Landau (GL) model is one of the most studied models physics, and it is applied as 'meta-model' in a wide range of fields[20]. The continuum version of the model is given by the functional integral

$$Z = \int \mathcal{D}A_\nu \mathcal{D}\phi \exp\left[- \int d^d x \left[\frac{1}{4} F_{\mu\nu}^2 + |(\partial_\nu + iqA_\nu)\phi|^2 + m^2|\phi|^2 + \lambda|\phi|^4 \right] \right]. \quad (16)$$

The parameter y is temperature like, driving the system through a phase transition, and x determines the importance of phase fluctuations versus amplitude fluctuations of the condensate field ϕ , see e.g. 29 for a more complete description of the various terms. For the present purpose the important is the following: For large values of x amplitude fluctuations ϕ are suppressed, the critical properties are dominated by phase fluctuations, and the transition is second order. In the limit $x \rightarrow 0$ the amplitude fluctuations dominate, and the transition is first order. For intermediate values of x all the degrees of freedom influence the dynamics, and for $x = x_T$ the transition changes order at a tricritical point[29].

In 2001 we determined the tricritical value x_T from large scale Monte Carlo simulations. Here we have re-analysed some of the data from this simulation, specifically we have studied one dataset with $x < x_T$, i.e. a

first order transition, and one dataset with $x > x_T$, i.e. a second order transition. Unfortunately the bulk of the simulations from 2001 were performed in the vicinity of x_T we therefor do not have any "extreme results".

Due to the problems mentioned in section IVD we are not able to calculate the overall normalisation g_0 of $g(\epsilon)$, nevertheless $g(\epsilon)$ shows the critical behaviour discussed in section IV B, and the behaviour of $F(y)$ clearly separates between first and second order transitions.

In conclusion we feel that in the application to the GL model the method has proved itself, and furthermore that it provides interesting information even though g_0 can not be determined.

Software to go through the steps described in sections II and III can be down-loaded as a C library from the authors web-site <http://www.ii.uib.no/~hove/libdos/>.

[1] Metropolis, N., A. W. Rosenbluth, M. N. Rosenbluth, A. H. Teller and E. Teller, J. Chem. Phys. **21**, 1087 (1953).

[2] SIAM News, volume 33, nr 4.

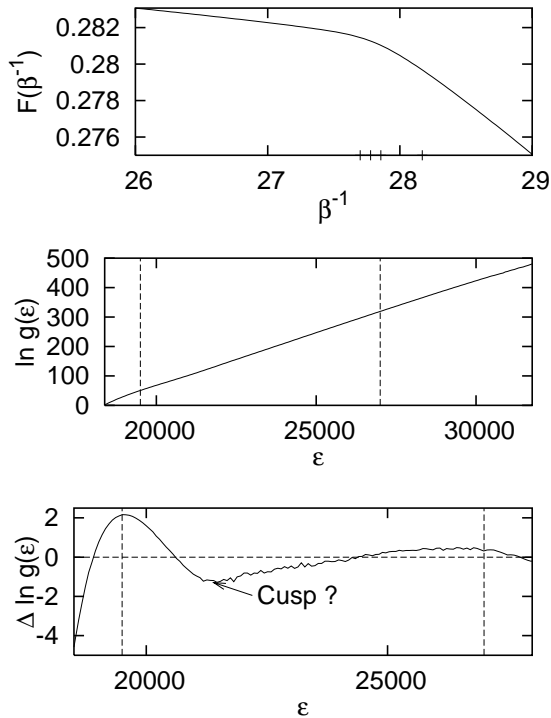


FIG. 9: The upper part shows the free energy $F(\beta)$, although it is rounded we can clearly see the remnants of a cusp in $F(\beta)$. The central figure shows $\ln g(\epsilon)$, the dashed lines indicate the two meta-stable energy levels ϵ_1 and ϵ_2 . In the lowest figure we have plotted $\ln g(\epsilon) - \hat{g}(\epsilon)$, where $\hat{g}(\epsilon)$ is a fit to a straight line on the interval $\epsilon_1 < \epsilon_2$. Although not very prominent, the structure in this plot is significant, see the discussion at the end of section IV B. The thin ticks on the x axis of the upper figure indicates the coupling where the simulations were performed, the results come from a simulation of a system of $40 \times 40 \times 40$ lattice units.

[3] J. E. Gubernatis (Editor), *THE MONTE CARLO METHOD IN THE PHYSICAL SCIENCES: Celebrating the 50th Anniversary of the Metropolis Algorithm*, Proceeding 690, AIP Publishing, (2003).
 [4] D. P. Landau and K. Binder, *A Guide to Monte Carlo Simulations in Statistical Physics*, Cambridge University Press, (2000).
 [5] B. J. Schulz, K. Binder and M. Mueller, *Int. J. Mod. Phys. C* **13**, 477 (2002), B. A. Berg, cond-mat/9909236 (1999), F. Wang and D. P. Landau, *Phys. Rev. Lett.* **61**, 2050 (2001).
 [6] F. Reif, *Fundamentals of statistical and thermal physics*, McGraw Hill, (1985).
 [7] K. Binder and D. W. Heermann, *Monte Carlo Simulations in Statistical Physics*, Springer Verlag, (1997).
 [8] A. E. Ferdinand and M. E. Fisher, *Phys. Rev.* **185**, 185 (1969).
 [9] M. Henkel, *Conformal Invariance and Critical Phenomena*, Springer Verlag, (1999).
 [10] H. W. J. Blöte, J. L. Cardy and M. P. Nightingale, *Phys. Rev. Lett.* **56**, 742 (1986).
 [11] I. Affleck, *Phys. Rev. Lett.* **56**, 746 (1986).
 [12] L. Onsager, *Phys. Rev.* **65**, 117 (1944).

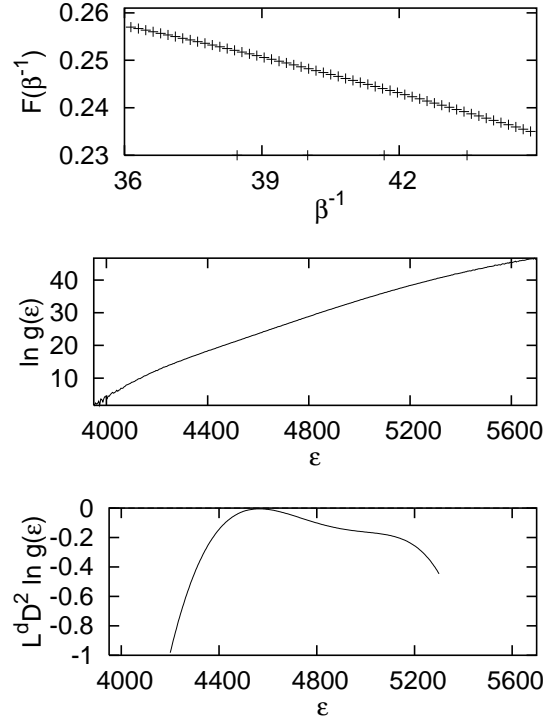


FIG. 10: The two upper panels show the same as Fig. 9, for a second order transition. The lower panel shows $\partial_\epsilon^2 \ln g(\epsilon)$, and we can see that this approaches zero at the critical energy $\epsilon_c \approx 4600$, this can be compared to Fig. 3

[13] D. A. Lavis and G. M. Bell, *Statistical Mechanics of Lattice Systems 2*, Springer Verlag, (1999).
 [14] J. Cardy, *Scaling and Renormalization in Statistical Physics*, Cambridge University Press, (1997).
 [15] M. Weigel and W. Janke, *Europhys. Lett.* **51**, 578 (2000).
 [16] V. Dotsenko, J. L. Jacobsen, M.-A. Lewis and M. Picco, *Nucl. Phys. B* **546**, 505 (1999).
 [17] S. Elizur, R. B. Pearson and J. Shigemitsu, *Phys. Rev. D* **19**, 3698 (1979).
 [18] Thomad Ramstad, Diploma Thesis, NTNU 2003.
 [19] J. Hove and A. Sudbø, *Phys. Rev. E* **68**, 046107 (2003).
 [20] Selected examples include the Higgs mechanism in particle physics [21], phase transitions in liquid crystals [22, 23], crystal melting [24], the quantum Hall effect [25, 26], superconductivity [27] and it is also used as an effective field theory describing phase transitions in the early Universe [28].
 [21] S. Coleman and E. Weinberg, *Phys. Rev. D* **7**, 1988 (1973).
 [22] P. G. de Gennes, *Solid State Commun.* **10**, 753 (1972).
 [23] T. C. Lubensky and J.-H. Chen, *Phys. Rev. B* **17**, 366 (1978).
 [24] H. Kleinert, *Gauge Fields in Condensed Matter*, World Scientific Publishing, (1989).
 [25] X. G. Wen and Y. S. Wu, *Phys. Rev. Lett.* **70**, 1501 (1993).
 [26] L. Pryadko and S. C. Zhang, *Phys. Rev. Lett.* **73**, 3282 (1994).
 [27] M. Tinkham, *Introduction to Superconductivity*, McGraw-Hill, (1996).

- [28] A. Vilenkin and E. P. S. Shellard, *Cosmic strings and other topological defects*, Cambridge University Press, (1994).
- [29] S. Mo, J. Hove and A. sudbø, Phys. Rev. B **65**, 104501 (2002).